IPMU09-0111
Preprint typeset using LaTeX style emulateapj v. 11/12/01

# DOES GALACTIC MAGNETIC FIELD DISTURB THE CORRELATION OF THE HIGHEST ENERGY COSMIC RAYS WITH THEIR SOURCES?

HAJIME TAKAMI[1] AND KATSUHIKO SATO[1,2]
hajime.takami@ipmu.jp
*IPMU09-0111*

## ABSTRACT

The propagation trajectories of the highest energy cosmic rays can be deflected by Galactic magnetic field (GMF) and expected correlation between their arrival directions and the positions of their sources can be disturbed. In order to explore whether the possible correlation is disturbed or not, we simulate the arrival distribution of the highest energy protons (HEPs) with energies above $6 \times 10^{19}$ eV taking 4 different GMF models into account and investigate the cross-correlation between the protons and sources assumed in the simulation. We show that the error of cross-correlation function adopted in this study is sufficiently small by accumulating 200 events. We also find that the correlation is not disturbed largely in many cases after 200 events accumulation and positive signals of the correlation are significantly expected at angular scale of 3-5°. Only in the cases of the northern sky with axisymmetric spiral structures of GMF, the cross-correlation functions are consistent with no correlation or have very low significance even if the correlation is positive at small angular scale. Conversely, no observation of the correlation within this scale implies no field reversal of GMF outside the solar system. Finally, we draw the possible source directions of recently published data of the Pierre Auger Observatory (PAO) assuming the composition to be purely protons and irons, and demonstrate that the pure-iron assumption may break the correlation of the PAO data with the large-scale structure of local Universe.

*Subject headings:* cosmic rays — methods: numerical — ISM: magnetic fields — Galaxy: structure

## 1. INTRODUCTION

The origin of the highest energy cosmic rays (HECRs) is one of the biggest mysteries in astrophysics. Although theoretical candidates of HECR sources have been proposed (for reviews, see Bhattacharjee & Sigl (2000); Torres & Anchordoqui (2004)), we have not found any source yet. A difficulty to find their sources is their deflections by intervening magnetic fields, i.e., Galactic magnetic field (GMF) and intergalactic magnetic field (IGMF). Since HECRs are charged hadrons, these magnetic fields deflect the trajectories of HECRs from their sources to the Earth.

Recent progress to construct HECR observatories with larger effective area has enabled us to accumulate a number of HECR events and to draw anisotropic distribution of HECR arrival directions (Takeda et al. 1999; Abraham et al. 2007, 2008). The anisotropy includes information on the positions of their sources and intervening magnetic fields from the sources to the Earth. Also, the Pierre Auger Observatory (PAO) found the correlation between the arrival directions of their 27 events above $5.7 \times 10^{19}$ eV and extragalactic astrophysical objects in local Universe within $z = 0.018$ and angular scale of 3.1° (Abraham et al. 2007, 2008). Several authors have also analyzed the PAO data since publishing their HECR data. George et al. (2008) showed a significant correlation of the PAO events with hard X-ray selected active galactic nuclei (AGNs) by using the 2 dimensional generalization of Kolmogorov-Smilnov test. More generally, the correlation with large-scale structure in the local Universe had been shown (Ghisellini et al. 2008; Kashti & Waxman 2008; Takami et al. 2009). Especially, Takami et al. (2009) showed that the separation angles between the arrival directions of HECRs and their sources are less than $\sim 15°$ by an analysis independent of specific source candidates, which bounds the deflection angles of HECRs in the local Universe. All these works indicate that the origin of HECRs is extragalactic objects related to the distribution of galaxies. Furthermore, in an optimistic view, we can interpret these results as an evidence that intervening magnetic fields are not as strong as information on the directions of their sources disappears like predictions by Dolag et al. (2005); Takami et al. (2006). (but see Sigl et al. (2004); Kotera & Lemoine (2008); Das et al. (2008); Ryu et al. (2009) for strong IGMF). This interpretation implies that much more accumulation of HECR events can unveil the positions of their sources as strongly concentrated events within a few degree, as demonstrated by Blasi & de Marco (2004) without considering any intervening magnetic field. Takami & Sato (2008a) showed that such a correlation is also predicted for the highest energy protons (HEPs) even considering a structured IGMF model, which reflects matter distribution of local Universe actually observed. We can regard these works as predictions of the PAO results. However, it is still under debate that astrophysical objects which correlate with the PAO events are really HECR sources because these objects have weaker activity than theoretically predicted source candidates (Moskalenko et al. 2009).

Very recently, the PAO reported that significance of the correlation reported in Abraham et al. (2007, 2008) decreased for their new data in the same analysis before, though the correlation is still significant (Hague et al. 2009). Thus, we should reconsider the correlation of HECRs and their sources, and the effect of intervening magnetic fields to possible correlation. The large deflection angles of HECRs could disturb the correlation. Possibilities are (i) GMF affects the deflections significantly (ii) the main composition of the HECRs is heavier than protons (iii) the IGMF model used in Takami & Sato (2008a) was optimistic, i.e., the deflections predicted by the IGMF model is smaller than that in the real universe. In this study, we focus on the possibility (i) assuming that the composition of HECRs

[1] Institute for the Physics and Mathematics of the Universe, the University of Tokyo, 5-1-5, Kashiwanoha, Kashiwa, Chiba 277-8568, Japan
[2] Department of Physics, School of Science and Engineering, Meisei University, 2-1-1, Hodokubo, Hino-shi, Tokyo 191-8506, Japan

are protons and IGMF subdominantly affects the deflections of HEPs. The other possibilities will be discussed subsequently.

Cosmic rays arriving at the Earth are inevitably affected by GMF. The importance has driven us to consider the propagation of HECRs in the Galactic space (Stanev 1997; Medina-Tanco et al. 1998; Harari et al. 1999; Kalashev et al. 2001; Alvarez-Muniz et al. 2002; Tinyakov & Tkachev 2002; Prouza et al. 2003; Yoshiguchi et al. 2004; Tinyakov & Tkachev 2005; Kachelriess et al. 2007; Takami & Sato 2008b). These works have mainly investigated their propagation itself in detail and have shown that predicted deflections of HEPs are less than $\sim 10^\circ$, the deflection angles highly depend on their arrival directions, and the apertures of HECR detectors to extragalactic space are distorted. Some of them guessed HECR sources using information on observed events and their trajectories in the Galactic space. However, they have not predicted possible signals to find their sources from the arrival distribution of HECRs. Yoshiguchi et al. (2003) simulated the arrival direction distribution of HEPs using plausible source distribution, taking their propagation in a GMF model into account, but they focused on only the auto-correlation of HEPs.

In this study, we focus on how do we see HEP sources in the arrival distribution of HEPs. We consider the cross-correlation between the arrival directions of HEPs and the positions of their sources by simulations taking their propagation in magnetized Galactic space into account. Since we know the positions of HEP sources in simulations, we can calculate cross-correlation functions between them. Cross-correlation function we adopt in this study can also estimate the angular separation scale of the correlation automatically.

This paper is laid out as follows: §2 is devoted to explain GMF models, a HEP source model, the calculation method of the arrival distribution of protons, and define cross-correlation function. In §3, the cross-correlation functions of simulated HEPs with their sources are calculated for several situations, and the results are interpreted and discussed. Finally, the possibilities of (ii) and (iii) are discussed, and we summarize this study in §4.

## 2. CALCULATION TOOLS

### 2.1. *GMF Models*

The structure of GMF is still controversial as briefly described in our previous paper (Takami & Sato 2008b). Thus, we also adopt 4 different and extreme models of GMFs fairly used in that work, which were originally proposed by Stanev (1997). Although we adopted a dipole magnetic field for a $z$ component of GMF in addition to its spiral component related to the spiral structure of Milky Way matter in Takami & Sato (2008b), we focus on only the spiral field in this study because there is no direct evidence for the dipole GMF. We briefly introduce the GMF models below.

The radial and azimuthal components of a spiral magnetic field in the Galactic plane are given by

$$B_{r_{||}} = B(r_{||},\theta)\sin p, \quad B_\theta = B(r_{||},\theta)\cos p, \tag{1}$$

where $r_{||}$ and $\theta$ are the distance from the Galactic center and azimuthal angle around the Galactic center, respectively. Note that $\theta$ is defined as increasing clockwise and $\theta = 0^\circ$ corresponds to the Galactic center. $p$ is the pitch angle of the spiral field in the neighborhood of the solar system, set to $p = -10^\circ$. We assume 2 spiral structures: axisymmetric (AS) and bisymmetric (BS), whose field strengths at a point $(r_{||},\theta)$ are written as

$$B(r_{||},\theta) = \begin{cases} b(r_{||})\cos\left(\theta - \beta\ln\frac{r_{||}}{r_0}\right) & : \text{BS} \\ b(r_{||})\left|\cos\left(\theta - \beta\ln\frac{r_{||}}{r_0}\right)\right| & : \text{AS}. \end{cases} \tag{2}$$

Here $\beta \equiv (\tan p)^{-1} = -5.67$ and $r_0 = 10.55$ kpc is the galactocentric distance of the location with maximum field strength at $l = 0^\circ$, which can be expressed as $r_0 = (R_\oplus + d)\exp\left[-(\pi/2)\tan p\right]$, where $R_\oplus = 8.5$ kpc is the distance of the solar system from the Galactic center and $d = -0.5$ kpc is the distance to the nearest field reversal from the solar system in the BS model. Negative $d$ means that the nearest field reversal takes place inside the solar system. Note that the AS model does not have any field reversals. $b(r_{||})$ is the radial profile of the strength of the magnetic field, modelled by

$$b(r_{||}) = B_0\frac{R_\oplus}{r_{||}}, \tag{3}$$

where $B_0 = 4.4\mu$G, which corresponds to $1.5\mu$G in the neighborhood of the solar system. In a region around the Galactic center ($r_{||} < 4$ kpc), the field is highly uncertain and therefore assumed to be constant and equal to its value at $r_{||} = 4$ kpc. The spiral field is assumed to be zero for $r_{||} > 20$ kpc.

For a magnetic field in the Galactic halo, we adopt an exponential decreasing model with two scale heights (Alvarez-Muniz et al. 2002),

$$B(r_{||},\phi,|z|) = B(r_{||},\phi)\begin{cases} \exp(-|z|) & : |z| \le 0.5 \text{ kpc} \\ \exp(\frac{-|z|}{4} - \frac{3}{8}) & : |z| > 0.5 \text{ kpc} \end{cases} \tag{4}$$

where the factor $\exp(-3/8)$ lets the field continuous on $z$. The parities of the spiral fields are represented as

$$B(r_{||},\phi,-z) = \begin{cases} B(r_{||},\phi,z) & : \text{S type parity} \\ -B(r_{||},\phi,z) & : \text{A type parity}. \end{cases} \tag{5}$$

The combination between the 2 spiral structures and 2 parities leads to 4 different GMF models. We adopt these 4 GMF models in this study.

### 2.2. *Source model of HEPs*

We consider HEP sources distributed to be compatible with the large-scale structure (LSS) of local Universe actually observed. The adopted GMF models reflect the structure of our Galaxy to some extent and the deflection patterns of HEPs are expected to be dependent on the arrival directions of them. Furthermore, the PAO results imply HEP sources distributed to be comparable with the LSS of local Universe (Abraham et al. 2007, 2008; Ghisellini et al. 2008; Kashti & Waxman 2008; Takami et al. 2009). Thus, such a source distribution is essential. A model used in this study is originally based on Takami et al. (2006). Here, the model is briefly explained.

In the model, we regard subsets of galaxies as HEP sources. We adopt Infrared Astronomical Satellite Point Source Redshift Survey (IRAS PSCz) catalog of galaxies (Saunders et al. 2000) to construct the local distribution of galaxies. The IRAS PSCz catalog matches our purpose well, since it is a flux-limited, uniform catalog and has very large sky coverage ($\sim 84\%$ on the whole sky). However, this catalog includes 2 selection effects: one is unobserved galaxies with fluxes below the flux-limit of the IRAS satellite. The other is $\sim 16$ % unobserved area which corresponds to mainly the Galactic plane. We correct these selection effects by using a luminosity function of the IRAS galaxies (Takeuchi et al. 2003). For the former effect, we add virtual galaxies with luminosities less than the observationally limited flux in the vicinity of original IRAS galaxies. On the other hand, we simply assume that galaxies are distributed

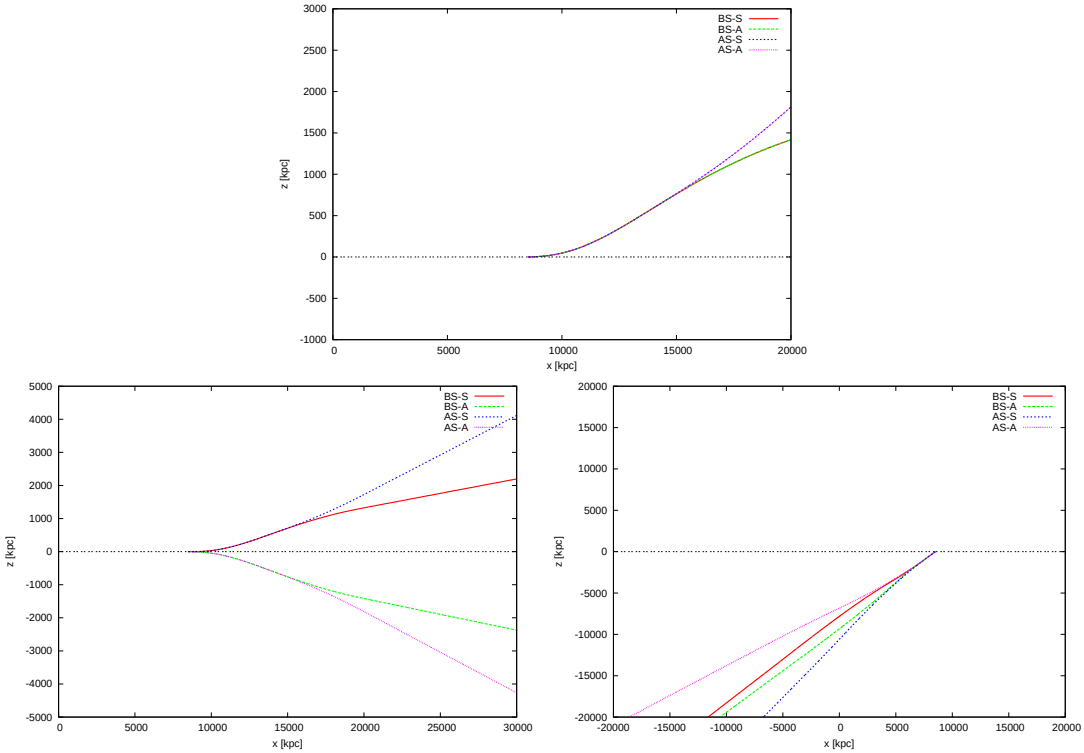


FIG. 1.— Examples of trajectories of protons with the energy of $10^{19.8} = 6.3 \times 10^{19}$ eV projected into a plane perpendicular to the Galactic disk and including the Galactic center and the Earth. Their arrival directions are $(\ell, b) = (180.0^\circ, 0.3^\circ)$ (*upper panel*), and $(180.0^\circ, -0.3^\circ)$ (*lower left panel*), and $(0.0^\circ, -44.8^\circ)$ (*lower right panel*), respectively. There are 4 trajectories of the protons in each panels, which correspond to trajectories in the BS-S (*red*), BS-A (*green*), AS-S (*blue*), and AS-A (*magenta*) GMF models.

isotropically for the latter one. Then, we randomly select galaxies according to a given number density of HEP sources, $n_s$, to make a subset of galaxies and regard it as a HEP source distribution. Such a structured source distribution is adopted up to 200 Mpc from our Galaxy because of the completeness of the IRAS PSCz catalog. Outside 200 Mpc, the distribution of HEP sources is assumed to be isotropic. We focus on HEPs above $6 \times 10^{19}$ eV in this study, 90% of which can reach the Earth from their sources within 200 Mpc . Thus, the isotropically distributed sources does not strongly affect our results.

For the physical properties of HEP sources, we assume that all the sources emit HEPs persistently with the same power with a power-law spectrum of $\propto E^{-2.6}$ whose index can well reproduce the observed spectrum of HECRs above $10^{19}$ eV. We consider 2 number densities of HEP sources, $n_s \sim 10^{-4}$ and $10^{-5}$ Mpc$^{-3}$. The former can best reproduce the anisotropy of the arrival distribution of HECRs observed by the PAO (Takami & Sato 2009; Cuoco et al. 2008). The latter is the number density to reproduce the AGASA anisotropy well (Takami et al. 2006; Blasi & de Marco 2004; Kachelriess & Semikoz 2005) and also is allowed by the PAO if plausible magnetic fields in the Universe are taken into account (Takami & Sato 2009).

### 2.3. *Simulation of Arriving HEPs*

In order to simulate the arrival distribution of protons for a given source distribution, this study adopts a calculation method developed by Takami et al. (2006). Generally, it costs much time to calculate arriving cosmic rays in a magnetized Universe because whether a cosmic ray injected from a source to a direction can reach the Earth is not known until its trajectory is calculated. Our method solved this problem and enables us to calculate the arrival distribution of protons taking their propagation in a magnetized space into account in reasonable CPU time.

In this method, we focus on an inverse process of propagation of protons. The trajectories of protons are calculated by the backtracking method. The trajectory of an oppositely-charged proton ejected from the Earth can regarded as that of a proton coming from extragalactic space. Many oppositely-charged protons (1,250,000 particles per logarithmic bin of energy in this study) are ejected from the Earth isotropically, and calculate their trajectories in the Galactic space. Once the particles escape from the Galactic space, they fly away straightforwardly with energy-*gain* until the comoving distances of the positions of the particles exceed 1,500 Mpc or the energy of the particles exceeds $10^{22}$ eV, which corresponds to the maximum injection energy of protons at sources, or the propagation time exceeds the age of the Universe. The boundary between the Galactic and extragalactic space is assumed to be 40 kpc from the Galactic center. We consider Bethe-Heitler pair creation, photopion production with cosmic microwave background (CMB) photons and adiabatic energy-loss due to the cosmic expansion as the energy-loss processes of HEPs in intergalactic space. We adopt $\Omega_m = 0.3$, $\Omega_\lambda = 0.7$, $H_0 = 71$ km s$^{-1}$ Mpc$^{-1}$ for the cosmological parameters. For photopion production, we adopt inelasticity and mean-free path calculated by an event generator SOPHIA (Mucke et al. 2000). The energy-loss is neglected in the Galactic space because all the energy-loss lengths of protons are much larger than the scale of the Galactic space.

When the trajectory of the $i$th oppositely-charged proton passes over sources, it obtains a weight for a positive arriving

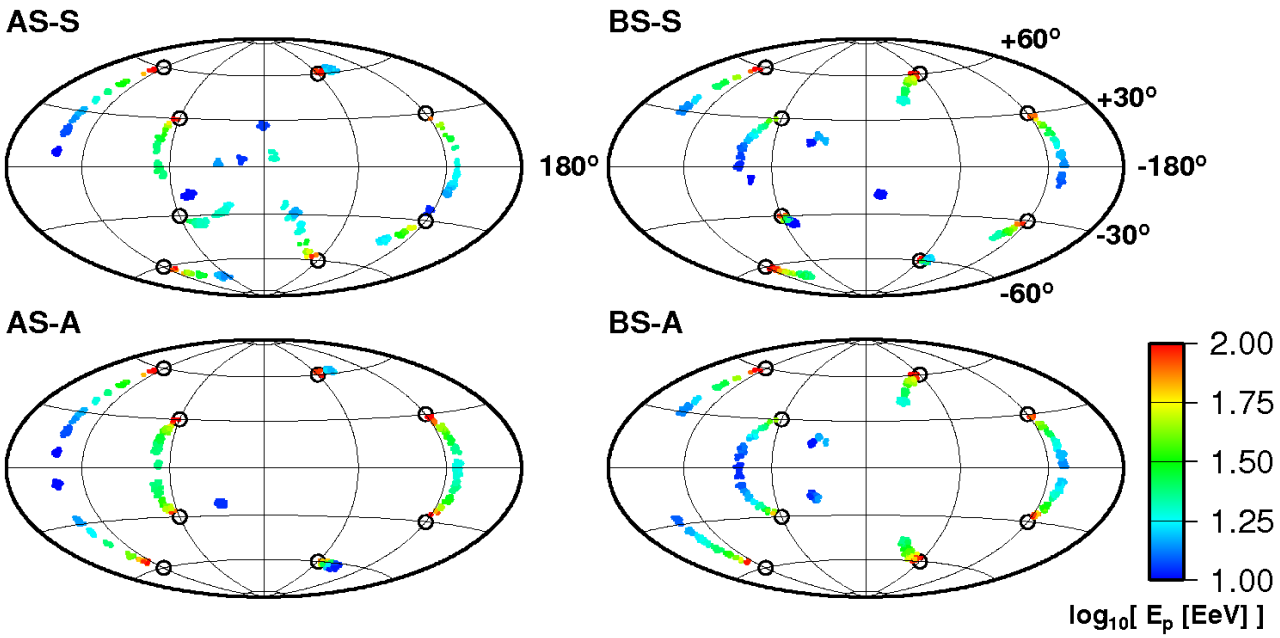


FIG. 2.— Arrival directions of HEPs with energies above $10^{19}$ eV emitted from sources located at 50 Mpc from the Earth (*black circles*) in Galactic coordinates. The energies of HEPs are represented in color. The 4 different GMF models are taken into account.

proton as,

$$P_{\rm selec}(E,i) \propto \sum_j \frac{1}{(1+z_{i,j})d_{i,j}{}^2} \frac{dN/dE_g(d_{i,j},{E_g}^j)}{E^{-1.0}} \frac{dE_g}{dE}, \quad (6)$$

where $j$ labels sources on the trajectory and a factor sums up for $j$. $z_{i,j}$ and $d_{i,j}$ are the redshift and comoving distance of the $j$th source, respectively. ${E_g}^j$ is the energy of the particle when it reaches the $j$th source. $dN/dE_g(d_{i,j},E_g) \propto {E_g}^{-2.6}$ is the spectrum of proton ejection of oppositely-charged protons at the $j$th source. $dE_g/dE$ can be calculated by the propagation data. $E^{-1.0}$ is the appearance of isotropic ejection with $dN/dlog_{10}E \propto$ const. from $10^{19}$ to $10^{21}$ eV. The weight corresponds to a relative probability in order that the $i$th particle is a really arriving proton. Thus, we randomly select the required number of trajectories from all the trajectories according to $P_{\rm selec}(E,i)$, and then arriving protons are obtained. The energy and arrival directions of the protons are the energy and the injection direction of corresponding oppositely-charged protons. We take the angular accuracy of HECR observatories to determine the arrival directions of HECRs. We assume that the arrival directions have a fluctuation described by a 2 dimensional Gaussian distribution with $\sigma = 1^\circ$, which corresponds to the angular accuracy.

### 2.4. *Statistical Methods*

We will discuss the correlation between the arrival directions of HEPs and their sources in the next section. Cross-correlation function for this purpose is defined as (Takami et al. 2009; Blake et al. 2006),

$$w_{es}(\theta) = \frac{ES(\theta) - ES'(\theta) - E'S(\theta) + E'S'(\theta)}{E'S'(\theta)}, \quad (7)$$

where the characters of $E$ and $S$ represent HEP events and their sources about which the cross-correlation is calculated, respectively. $ES(\theta)$ is the number of pairs between $E$ and $G$ with the separation angles from $\theta$ to $\theta+\Delta\theta$ divided by $N_eN_s$ for normalization, where $N_e$ and $N_s$ are the total numbers of the events and sources considered, respectively. $\Delta\theta$ is set to be $1^\circ$. $E'$ and $G'$ represent HEP events and sources randomly distributed following the apertures of HECR observatories and observations of HECR sources, respectively. $EG'(\theta)$, $E'G(\theta)$, and $E'G'(\theta)$ have similar meanings to $EG(\theta)$. $E'$ and $G'$ correct their non-uniform apertures. Note that the apertures of HEP sources is uniform in this study (see §2.2). By definition, $w(\theta) > 0$ means positive correlation.

The aperture of a ground array is simply described as (Sommers 2001)

$$\omega(\delta) \propto \cos(a_0)\cos(\delta)\sin(\alpha_m) + \alpha_m \sin(a_0)\sin(\delta), \quad (8)$$

where $\alpha_m$ is given by

$$\alpha_m = \begin{cases} 0 & \text{if } \xi > 1 \\ \pi & \text{if } \xi < -1 \\ \cos^{-1}(\xi) & \text{otherwise} \end{cases} \quad (9)$$

and

$$\xi \equiv \frac{\cos(\theta) - \sin(a_0)\sin(\delta)}{\cos(a_0)\cos(\delta)}. \quad (10)$$

Here, $a_0$ and $\theta$ are the terrestrial latitude of a ground array and the zenith angle for an experimental cut. We simulate the apertures of 2 HECR observatories; the PAO and Telescope Array (TA). The PAO observes the southern sky and the TA observes the northern sky. As we will see in §3.1, the deflection patterns of HEPs in the southern sky are quite different from those in the northern sky. The different signals of correlation between HECRs and their sources are expected. Thus, we consider the apertures of these observatories as representatives of HECR observatories in the southern and northern sky. The parameters are $a_0 = -35.2^\circ$ and $\theta = 60^\circ$ for the PAO (Abraham et al. 2008), and $a_0 = 39.3^\circ$ and $\theta = 45^\circ$ for the TA (Nonaka et al. 2009).

## 3. RESULTS

### 3.1. *Deflections of protons by GMF*

First of all, we briefly view the trajectories and deflections of HEPs by GMF. The 4 GMF models predict different trajectories

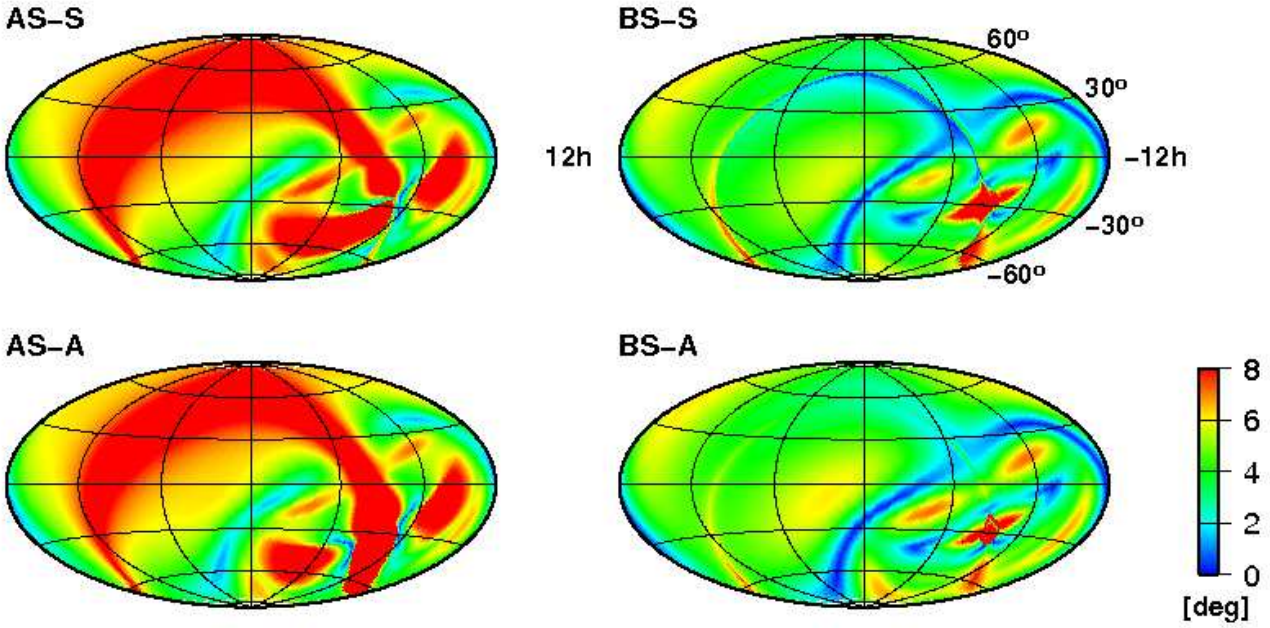


FIG. 3.— Deflection angles of arriving protons with energies of $10^{19.8}$ eV in color. The arrival directions are shown in equatorial coordinates. The difference between the AS GMF models and BS GMF models is obvious in the northern hemisphere.

of HEPs, since they are different in field reversals and parities above and below the Galactic plane.

Fig. 1 shows the trajectories of protons with the energy of $10^{19.8}$ eV and the same arrival directions in 4 GMF models. Practically, we eject oppositely-charged protons from the Earth and plot their trajectories. In order to see the effects of different GMF models, we select 3 examples of the arrival directions of protons. In the upper panel, we draw the trajectories of protons with the arrival direction of $(\ell, b) \sim (180.0^\circ, 0.3^\circ)$. The trajectory of a proton propagating in the BS-S (AS-S) GMF model is the same as that in the BS-A (AS-A) GMF model, since a spiral field in the BS-S (AS-S) model is, by definition, the same as that in the BS-A (AS-A) model above the Galactic plane. The trajectories of protons are the same both in the S models and in the A models as long as they propagate above the Galactic plane. The trajectories of the protons in the BS models are separated from those in the AS models just outside 15 kpc because of a field reversal of GMF. Once a proton passes over a field reversal, its deflection direction is changed into the opposite direction and the total deflection is weaken. This mechanism works only in the BS models. Thus, generally, the BS models predict smaller deflections of HECRs than the AS models. Once oppositely-charged protons propagate away from the Galactic plane, their deflections become smaller because a magnetic field becomes exponentially smaller. Therefore, the spiral structure of GMF just in the vicinity of the solar system mainly affects the deflections of HEPs.

We can see the effect of the parity of GMF in the other panels. The trajectories of protons with the arrival directions of $(\ell, b) = (180.0^\circ, -0.3^\circ)$ are described in the lower left panel. The trajectories of oppositely-charged protons are deflected toward the upside of the Galactic plane near the solar system in the case of GMF models with the S-type parity. On the other hand, their trajectories are deflected toward the downside of the Galactic plane for the A-type parity. Note that the magnetic structure of the BS-S (BS-A) model is the same as that of the AS-S (AS-A) model until the first field reversals inside and outside the solar system. The trajectories of the oppositely-charged protons are also separated at $\sim 15$ kpc due to a field reversal of GMF. The lower right panel, in which the arrival directions of HEPs considered are $(\ell, b) = (0.0^\circ, -44.8^\circ)$, is another example that HEP trajectories with the same arrival direction are separated by different GMF models.

The deflection directions of HECRs highly depend on the positions of their sources, their energies, and of course GMF structure. Fig. 2 demonstrates the arrival directions of protons above $10^{19}$ eV emitted from 8 extragalactic sources located at artificial positions shown by *black* circles to see the directions and strengths of their deflections. The energies of arriving protons are represented in color and the distance of sources is 50 Mpc.

We can see the dependency of the deflection angles on the positions of HEPs. For instance, protons from a source with $(\ell, b) \sim (-60^\circ, 60^\circ)$ are little deflected even for $\sim 10^{19}$ eV in the cases of the AS GMF models. Even for the BS models, the protons with energies of $\sim 10^{19}$ eV are deflected by $\sim 20^\circ$. On the other hand, the deflections of protons from a source with $(\ell, b) \sim (120^\circ, 60^\circ)$ are much larger for their energies of $\sim 10^{19}$ eV.

The arrival directions of protons from a source are arranged reflecting their energies and the GMF structure of the source direction (Yoshiguchi et al. 2003). The A-type parity leads to a symmetric structure of deflection pattern of HEPs. This arrangement structure of the arrival directions of protons can be a hint to understand the GMF structure of the source directions. When we focus on protons with lower energies, some events are highly deflected and then their arrival directions do not reflects the positions of their sources. Furthermore, a large fraction of such protons is contribution from cosmologically distant sources, and they work as background. So, the lower energy component of the arrangement is hidden. On the other hand, since the highest energy component of protons (*red points*) reaches the Earth only from nearby Universe because of Greisen-Zatsepin-Kuz'min (GZK) effect (Greisen 1966; Zat-

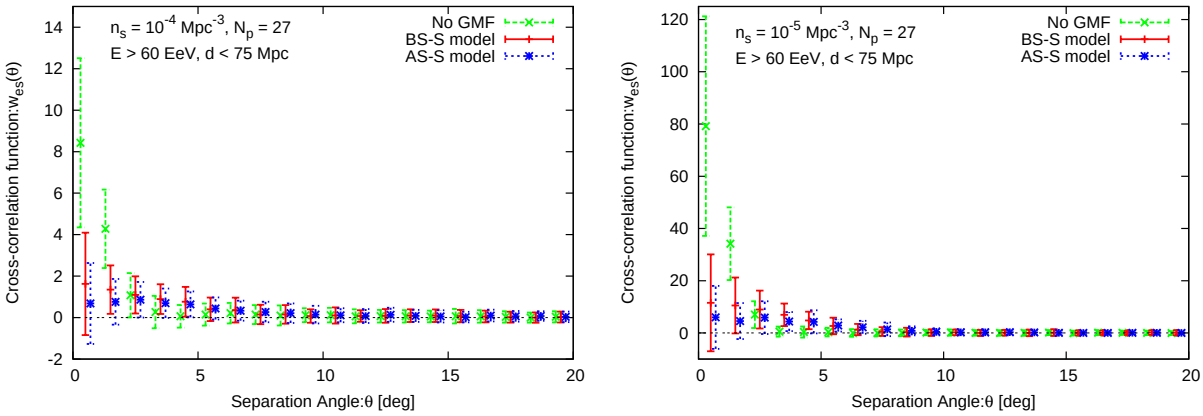


FIG. 4.— Cross-correlation functions between the positions of HEP sources within 75 Mpc and the arrival directions of simulated HEPs above $6 \times 10^{19}$ eV in the cases of $n_s \sim 10^{-4}$ (*left*) and $10^{-5}$Mpc$^{-3}$ (*right*). The number of the protons is set to be 27 events and the aperture of the PAO is taken into account. These functions are calculated under no GMF (*green*), the BS-S model (*red*), and the AS-S model (*blue*).

sepin & Kuz'min 1966), their arrangement is expected to be more clear, although the deflection angles are small. Such a component could be used to investigate GMF structures due to their small (but not too large) deflections. Also, such small deflections are useful to investigate their sources. Thus, we focus on the highest energy component of cosmic rays.

Finally, we see the distribution of the deflection angles of HEPs. in the terrestrial sky. Fig. 3 shows the deflection angles of protons arriving at the Earth with energies of $10^{19.8}$ eV in equatorial coordinates. We can find that GMFs with the AS structure predict larger deflection than those with the BS structure, as we discussed on Fig. 1. The difference between the AS models and BS models is noticeable in the northern sky. Thus, we can predict that the correlation of HEPs and their sources is quite different between the AS and BS GMF models in the northern sky. Note that the large deflection drawn in the lower right parts of all panels is generated by a strong magnetic field near the Galactic center.

### 3.2. *Cross-correlation with HEP sources*

Firstly, we see the effect of GMF to the cross-correlation. Fig. 4 shows the cross-correlation functions between the positions of sources within 75 Mpc and the arrival directions of simulated protons with energies above $6 \times 10^{19}$ eV in the cases of $n_s \sim 10^{-4}$ (*left*) and $10^{-5}$Mpc$^{-3}$ (*right*). The number of protons is set to that of the published PAO events (27 events). Also, the anisotropic aperture of the PAO is taken into account. These cross-correlation functions are calculated for unmagnetized Galactic space (*green*), the BS-S GMF model (*red*), and the AS-S GMF model (*blue*). These cross-correlation functions are calculated as follows; We simulate an arrival distribution of a required number of HEPs for a given source distribution. The arrival distribution and the source distribution enable us to calculate cross-correlation function. We realize 100 source distributions with the same $n_s$ following the method of §2.2 and calculate cross-correlation function in the same way for each of them. Finally, we calculate the average and standard deviation of the 100 cross-correlation functions and plot them as points and error bars, respectively. Therefore, the error bars include not only errors due to the finite number of simulated events but also errors originating from the uncertainty of HEP source positions, i.e., the uncertainty of galaxy sampling in our HEP source model. We can find that the correlation signals at small angular scale are suppressed by GMF. Note that a finite accuracy to determine the arrival directions of HEPs considered leads to positive values of the cross-correlation functions for no GMF at the second and third bins.

When we consider a smaller number density of HEP sources, the absolute values of the cross-correlation functions become larger. However, the error bars of the cross-correlation functions also become larger because the uncertainty of source positions is larger. Thus, statistical features are little changed by $n_s$.

Next, we simulate a current status of the PAO for 4 GMF models. Fig. 5 shows the cross-correlation functions of HEP sources within 75 Mpc and protons above $6 \times 10^{19}$ eV simulated for the BS-S (*red*), BS-A (*green*), AS-S (*blue*), and AS-A (*magenta*). The number of protons is assumed to be 27. We take the aperture of the PAO into account in the left panel. For comparison, the aperture of the TA is considered in the right panel.

In the left panel, all the cross-correlation functions are not consistent with a lack of the correlation at a few degree within standard deviations, though at the first and second bins these are consistent with zero because large error bars. Thus, the correlation of HEPs and their sources is expected with a few degree separation even at present. It is remarkable that the angular separation of the correlation is comparable with the the correlation scale by the PAO (3.1°).

We can find the difference of cross-correlation signals between GMF models in the northern sky (*right panel*). The predictions of the AS models are consistent with no correlation, while the BS models predict positive correlation at a few degree like the case of the southern sky. This difference is an appearance of the difference of the deflection angles of HEPs between the AS and BS GMF models, as we have seen in Fig. 3. We can also see that the 2 BS models (or the 2 AS models) predict quite similar cross-correlation functions. This means that the difference between the S-type parity and A-type parity does not appear on the cross-correlation function. Although the difference between the parities is the deflection directions of HEPs as we saw in Fig. 2, the cross-correlation function does not include information on the deflection directions. These features will be more clear by accumulating more events as discussed subsequently.

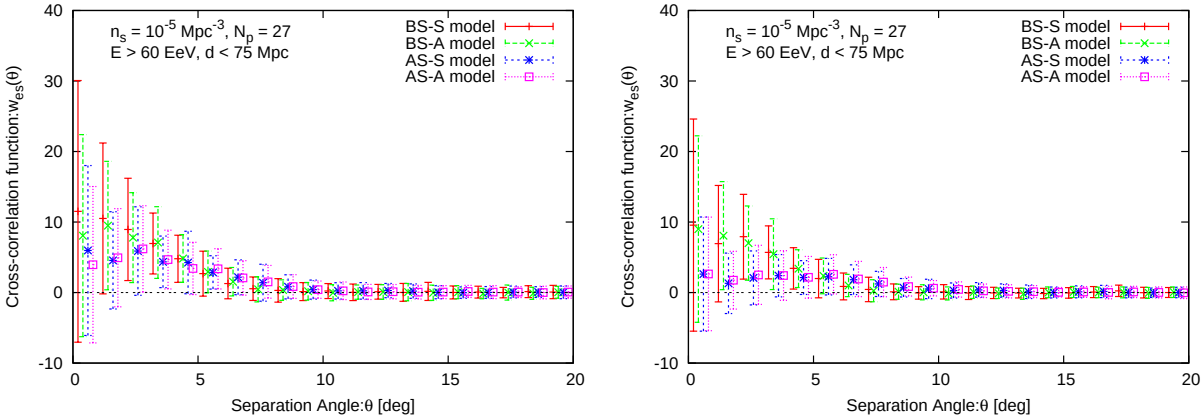


FIG. 5.— Cross-correlation functions of 27 protons for the 4 GMF models with energies above $6 \times 10^{19}$ eV and their sources within 75 Mpc. $n_s = 10^{-5}$ Mpc$^{-3}$ is assumed. The anisotropic apertures of the PAO (*left*) and TA (*right*) are taken into account.

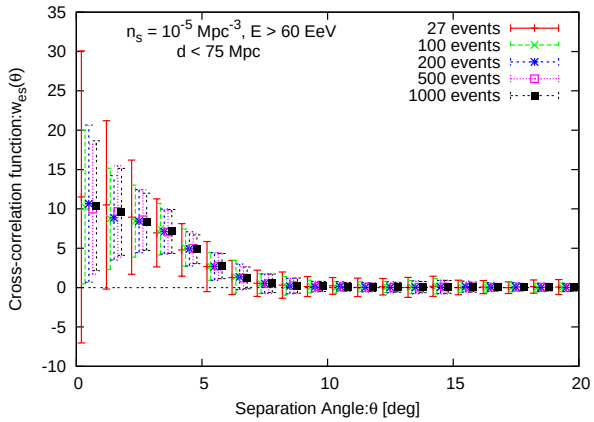


FIG. 6.— Cross-correlation functions between HEPs simulated in the BS-S GMF model with energies above $6 \times 10^{19}$ eV and their sources within 75 Mpc. $n_s = 10^{-5}$ Mpc$^{-3}$ is assumed. The numbers of simulated protons are 27 (*red*), 100 (*green*), 200 (*blue*), 500 (*magenta*), and 1000 (*black*), respectively. The decrease of error bars is saturated at $\sim$ 200 protons.

The error bars of the cross-correlation functions originate from not only the finite number of events but also the uncertainty of positions of HECR sources (i.e., the uncertainty of sampling galaxies in our source model). We can decrease the former errors by increasing the number of observed events, whereas the latter type of errors cannot be reduced because we do not know any source at present. For an ideal case where the number of detected events is infinite, we can consider only the latter errors. Practically, it is meaningful to estimate the number of events for saturation of the errors because we can discuss the correlation of HEPs and their sources based on almost only the uncertainty of the precise positions of the sources after the accumulation of such number of events. Fig. 6 shows the cross-correlation functions between HEP sources within 75 Mpc and arriving protons simulated for the BS-S GMF model on the assumption of the PAO aperture. The numbers of protons considered are 27 (*red*), 100 (*green*), 200 (*blue*), 500 (*magenta*), and 1000 (*black*). When the number of events is small, errors due to the finite number of events occupy a significant fraction of the total errors. As increasing the number of events, the errors decreases and errors due to the sampling of galaxies are dominated. An estimation by eye implies that the total errors are sufficiently saturated by $\sim$ 200 events detection. This is unchanged for other $n_S$, GMF models, and the northern sky. Thus, we consider 200 events for discussions below. If we observe the positive value of cross-correlation function after 200 event accumulation, it means that positive correlation between HEPs and their sources is expected even if the uncertainty of HEP source positions is taken into account.

Fig. 7 shows the cross-correlation functions of 200 protons with energies above $6 \times 10^{19}$ eV and their sources for the BS-S (*red*), BS-A (*green*), AS-S (*blue*), and AS-A (*magenta*). The assumed number density of the sources is $\sim 10^{-5}$ Mpc$^{-3}$. The apertures of the PAO (*left*) and TA (*right*) are taken into account. We can see the results of Fig. 5 more clearly because of the smaller errors.

In the left panel, all the 4 GMF models predict the positive correlation within standard deviations at small angular scale. Thus, the correlation between HEPs and their sources is predicted despite the uncertainty of the source positions in the southern sky. Separation angles of which significance is the highest is 3° and 4° for the BS models and the AS models, respectively. Separation angles at which positive correlation is predicted are smaller in the BS models than in the AS models, reflecting the difference of the deflection angles of HEPs. They are also up to $\sim 6°$.

On the other hand, the predictions of the BS models are different from those of the AS models in the northern sky. In the right panel, the cross-correlation functions calculated for the AS models are consistent with no correlation within $\sim 3°$ within standard deviations, whereas the cross-correlation functions are significantly positive for the BS models at the same angular scale . At larger angular scale, the cross-correlation functions are slightly positive for the AS models, but the significance is quite low. Thus, the predictions of the AS GMF models are almost consistent with no correlation. Since the difference between the BS and AS models is based on the existence of field reversals, observations of very weak or no correlation at the small angular scale imply no field reversals outside the solar system.

We can see the difference between the BS and AS GMF models more obviously by demonstrating the cross-correlation functions calculated from a given source distribution with $\sim 10^{-5}$ Mpc$^{-3}$, shown in Fig. 8. The apertures of the PAO (*left*) and TA (*right*) are considered. We realize the arrival distribution of 200 HEPs 100 times from the source distribution, calculate a cross-correlation function for each of them, and estimate the average and standard deviation of the 100 cross-correlation functions. Thus, the error bars originate from only the finite

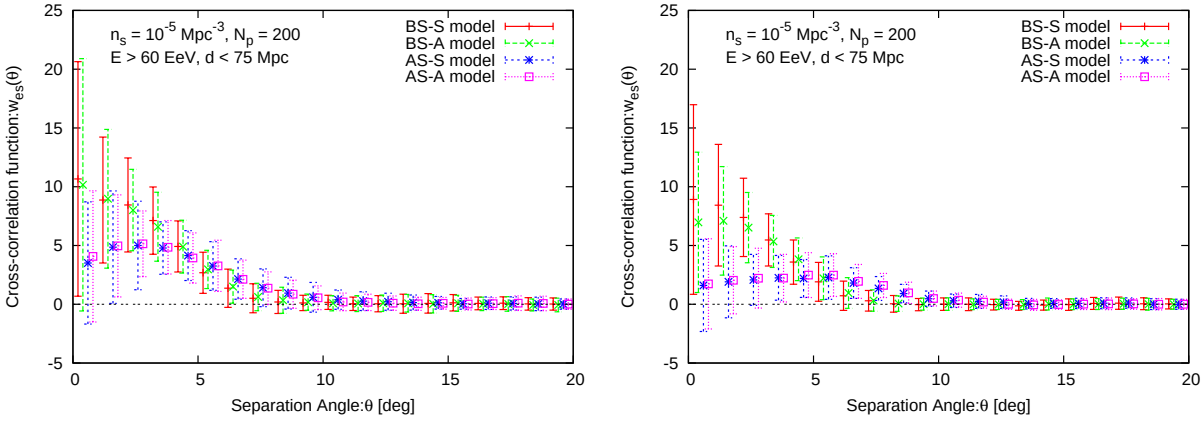


FIG. 7.— Cross-correlation functions between 200 protons simulated for the 4 GMF models with energies above $6 \times 10^{19}$ eV and the positions of their sources within 75 Mpc in the case of $\sim 10^{-5}$ Mpc$^{-3}$. The apertures of the PAO (*left*) and TA (*right*) are taken into account.

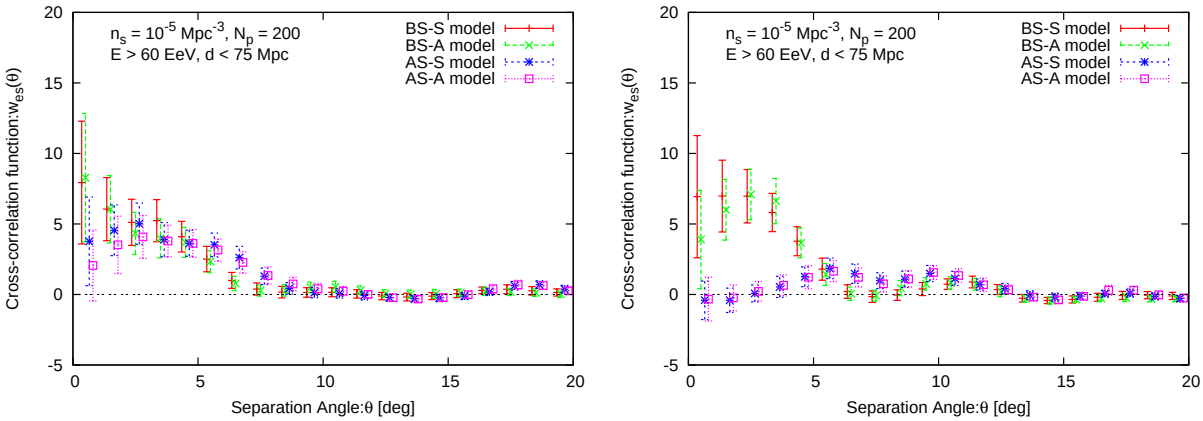


FIG. 8.— Cross-correlation functions between 200 protons simulated from a source distribution with $n_s \sim 10^{-5}$ Mpc$^{-3}$ with energies above $6 \times 10^{19}$ eV and the positions of their sources within 75 Mpc from the Milky Way The apertures of the PAO (*left*) and TA (*right*) are taken into account.

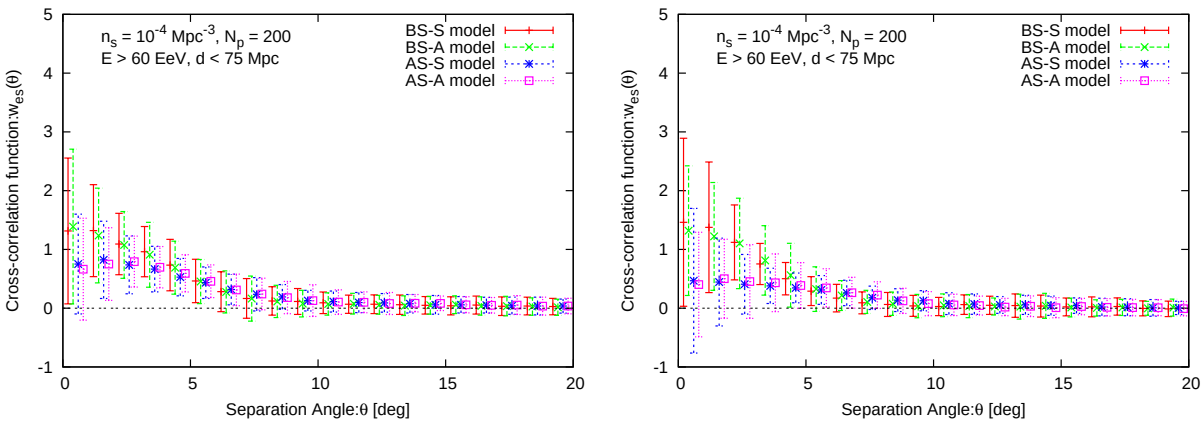


FIG. 9.— Same as Fig. 7, but for $n_s \sim 10^{-4}$ Mpc$^{-3}$.

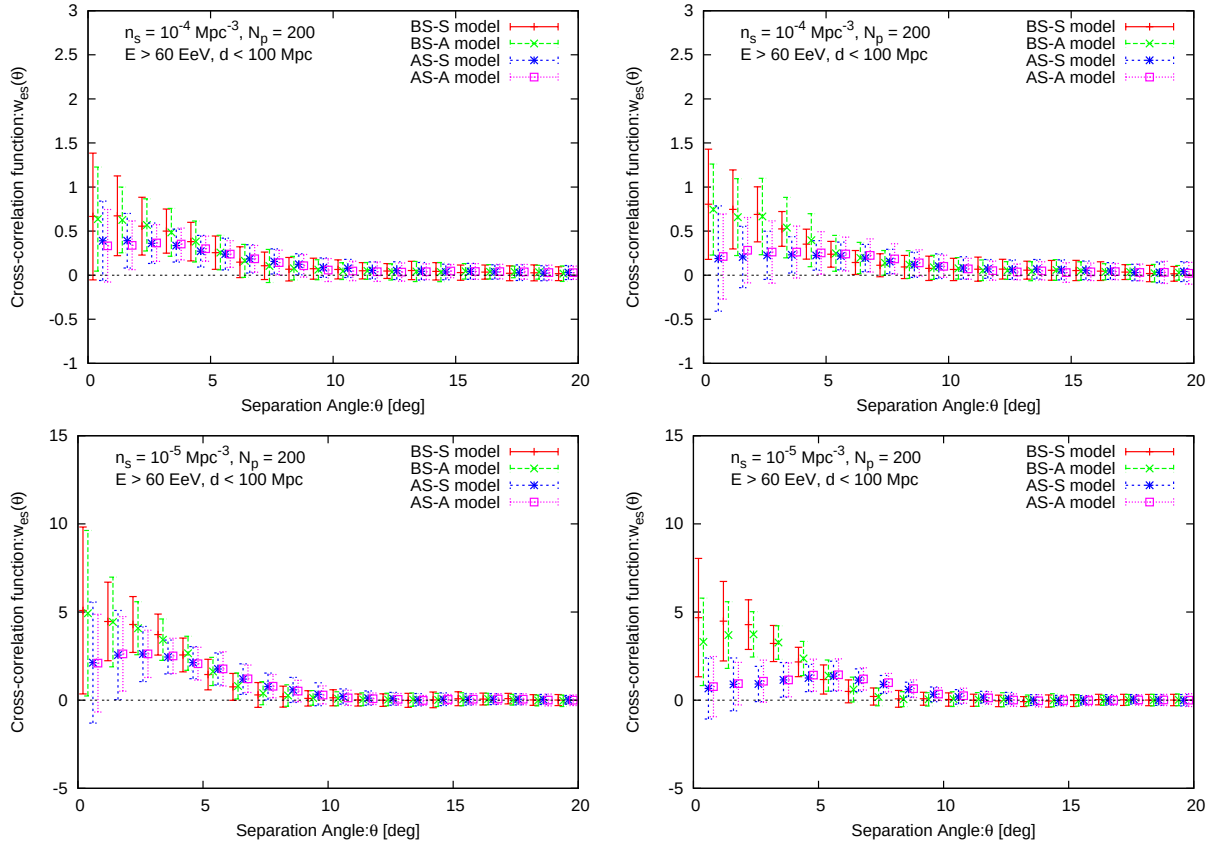


FIG. 10.— Cross-correlation functions of 200 protons simulated for the 4 GMF models with energies above $\sim 6 \times 10^{19}$ eV and the positions of their sources within 100 Mpc. $n_s \sim 10^{-4}$ Mpc$^{-3}$ (*upper panels*) and $n_s \sim 10^{-5}$ Mpc$^{-3}$ (*lower panels*) are assumed. The anisotropic apertures of the PAO (*left panels*) and TA (*right panels*) are taken into account.

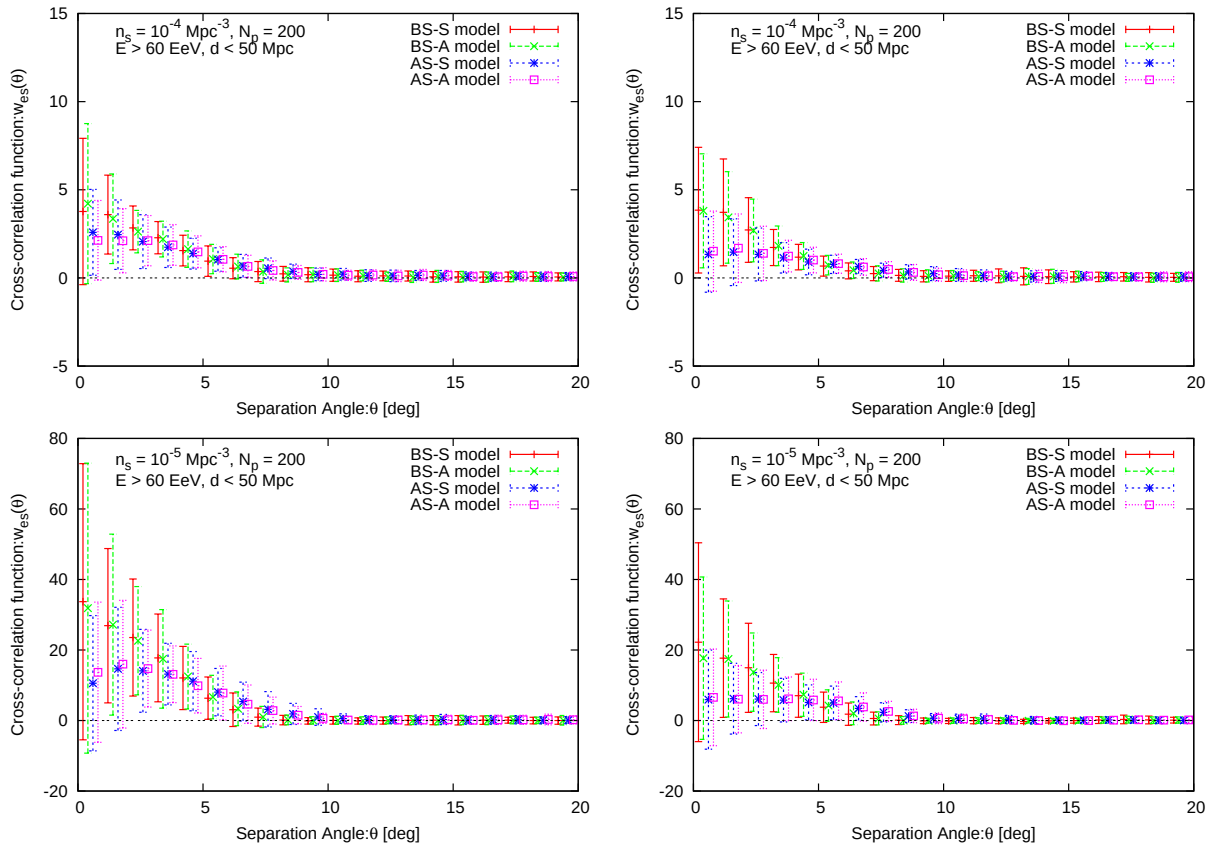


FIG. 11.— Same as Fig. 10, but for HEP sources within 50 Mpc.

number of events. While all the 4 GMF models show similar cross-correlation functions with significantly positive signals at small angular scale in the southern sky, cross-correlation functions are clearly different between the AS and BS GMF models in the northern sky. In this example, the BS models predict strongly positive correlation, but the cross-correlation functions derived from the AS models are consistent with zero at small angular scale.

When we consider larger number density of HEP sources, the values of the cross-correlation function become smaller at small angular scale as seen in Fig. 5. Nevertheless, the qualitative features of the cross-correlation functions are unchanged. Fig. 9 shows the same figure as Fig. 7, but the number density of the sources is $\sim 10^{-4}$ Mpc$^{-3}$. The significance and angular scale of positive correlation is similar to the cases of $n_s \sim 10^{-4}$ Mpc$^{-3}$.

So far, we have fixed the maximum distance of HEP sources considered for correlation as 75 Mpc, which is the same distance as analyses by the PAO (Abraham et al. 2007, 2008) ( $z = 0.018$ in the concordance cosmology ). However, this value was derived to optimize the correlation signal, and therefore it does not have inevitability, although it is not inconsistent with the GZK scenario. Thus, we check the correlation by changing the maximum distance considered, adopting 100 Mpc and 50 Mpc.

Fig. 10 shows the cross-correlation functions of 200 protons with energies above $6 \times 10^{19}$ eV and their sources within 100 Mpc. $n_s \sim 10^{-4}$ Mpc$^{-3}$ (*upper panels*) and $n_s \sim 10^{-5}$ Mpc$^{-3}$ (*lower panels*) are assumed. The anisotropic apertures of the PAO (*left panels*) and TA (*right panels*) are taken into account. Compared to Figs. 7 and 9, qualitative features are the same, that is, positive correlation is predicted at small angular scale except for the AS GMF models in the northern sky. The exception shows the cross-correlation functions almost consistent with no correlation. Fig. 11 shows the same as Fig. 10, but the maximum distance of HEP sources considered for correlation is 50 Mpc. They have also the same qualitative features as Fig. 10. However, we can find that the significance of positive correlation is lower than in Figs. 7, 9 and 10, because of relatively large error bars. A main reason of this is a smaller volume including considered sources. Since the number of sources used for correlation analysis is small, the fluctuations of the cross-correlation functions become large. Thus, the investigation of spatial correlation with nearby sources is not always efficient. On the other hand, considering distant sources is also not always better because there are the deflections of HEP trajectories by IGMF, which has much uncertainty, in a real situation. Therefore, the maximum distance of sources with which the correlation is considered should be treated as a parameter at present, when we analyze observational data actually.

## 4. DISCUSSION & CONCLUSION

In this study, we considered the propagation of HEPs in the Galactic space and investigated the cross-correlation between the arrival directions of HEPs with energies above $6 \times 10^{19}$ eV and the projected positions of their sources by using simulations. We found that the expected correlation between HEPs and their sources is not disturbed and is positive at small angular scale in many cases after 200 HEPs detection, although a coherent (spiral) component of GMF efficiently deflects the

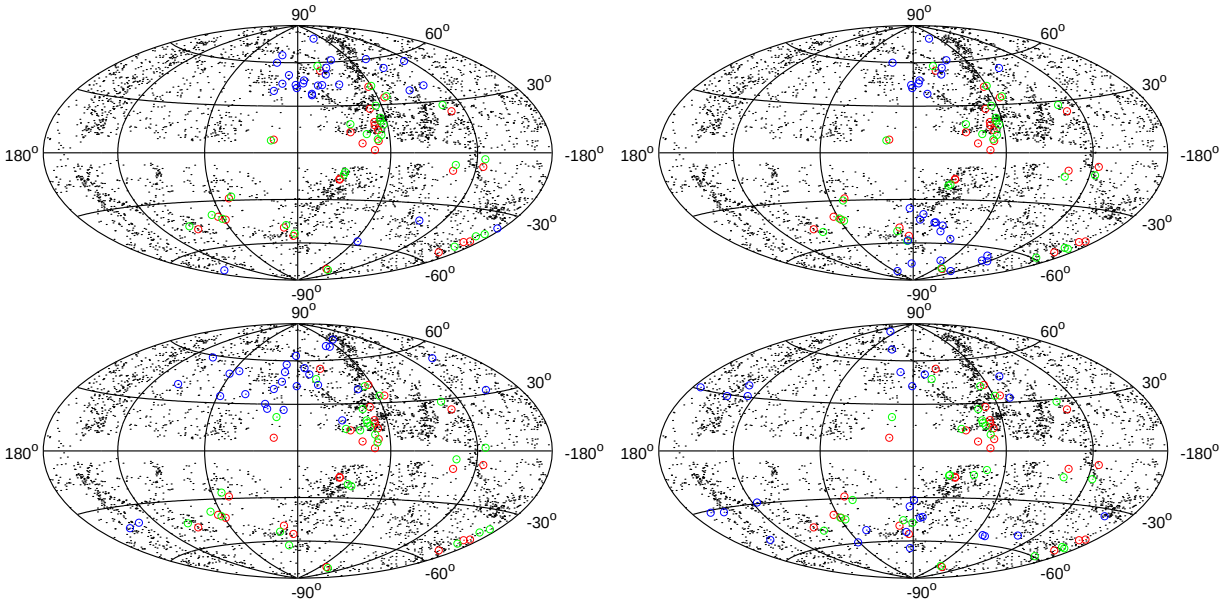


FIG. 12.— Arrival directions of the PAO events published in Abraham et al. (2008) (*red*) and the possible directions of their sources on the assumption that all the PAO events are protons (*green*) and irons(*blue*). In other words, we backtrack the PAO events following the BS-S model (*upper left*), BS-A model (*upper right*), AS-S model (*lower left*), and AS-A model (*lower right*), and plot their velocity directions at the boundary between the Galactic space and extragalactic space.

trajectories of HEPs. An exception is the cases of the AS GMF models in the northern sky. In these cases, the predicted cross-correlation is consistent with no correlation or has very low significance even if it is positive, which reflects that the BS models predict the smaller deflections of HEPs than the AS models especially in the northern sky. Since the difference of the deflection angles is produced by field reversals of GMF, null observation of the correlation between HEPs and their sources or very weak correlation imply no field reversals of GMF at least outside the solar system. These features are qualitatively unchanged if we change the maximum distance of HEP sources with which we consider the correlation in the range within 100 Mpc.

Finally we discuss 3 points which are able to affect the results of this study; the compositions of HECRs (possibility (ii) listed in §1), GMF in the Galactic halo, and intergalactic magnetic field (possibility (iii) listed in §1). Recent reports of the PAO showed that HECRs include a large fraction of the heavier nuclei by $< X_{\rm max} >$ and the deviations of $X_{\rm max}$ measurements (Bellido et al. 2009) (although the HiRes reported proton-dominated composition at the highest energy (Belz et al. 2009)). A remarkable point is that the PAO simultaneously reported that the correlation between the arrival directions of HECRs and the positions of nearby astrophysical objects (Abraham et al. 2007, 2008; Hague et al. 2009). Since the trajectories of heavy nuclei are more deflected by intervening magnetic fields than protons, the observed spatial correlation tends to be disturbed if heavy nuclei are included in observed HECRs.

It is expected from a reaction with CMB photons that the main component of heavy nuclei in HECRs is iron. Nuclei can be broken through giant dipole resonance by interactions with CMB photons at ultra-high energy. The giant dipole resonance predicts a GZK-like spectral steepening, but the energy of steepening is lower than the GZK steepening because its threshold energy is smaller than that of photopion production of protons (e.g., Allard et al. (2005)). The energy of the steepening by the giant dipole resonance increases as increasing the atomic number of nuclei, and then the energy becomes comparable with the energy of the GZK steepening. Thus, the dominant component of heavy nuclei in HECRs should be irons to fit an observed energy spectrum with the GZK-like feature. Lighter nuclei disturb such a spectral shape. Compositions other than protons and irons must be a very small fraction. It is quite serious for the spatial correlation observed by the PAO.

In Fig. 12, we demonstrate that source positions of the PAO events with the IRAS galaxies within $z = 0.018$ (*black dots*) assuming that all of the PAO events are protons (*green*) and irons (*blue*). We backtrack the detected PAO events (*red*) in the 4 GMF models and plot their velocity directions just outside the Galaxy (at 40 kpc from the Galactic center). These circles represent the intrinsic directions of their sources on the assumption of no IGMF. We can obviously find that the inferred directions of iron sources are not consistent with the distribution of nearby galaxies. It is a fine-tuning problem that the deflection by IGMF improves the correlation. Thus, pure iron scenario is problematic in the viewpoint of the spatial correlation. In order to satisfy the consistency of the results of composition measurements and the spatial correlation observed by the PAO, HECRs also include significant fraction of protons. The proton component can unveil the positions of HEP sources as we have shown in this study. In this viewpoint, the fraction of irons to protons is an essential quantity to explain the current result of the PAO.

We consider only spiral fields of GMF in this study. However, vertical components (perpendicular to the Galactic Plane) of GMF have been observed both in the vicinity of the solar system (Han & Qiao 1994) and around the Galactic center (Han 2007). A magnetic field in the Galactic halo might also affect the deflections of HECR trajectories. The existence of Galactic wind has been indicated by Galactic diffuse soft X-ray observations (Everett et al. 2008). On the other hand, high-sensitivity observations of several edge-on galaxies with galactic winds have revealed so-called X-shaped magnetic fields in their halos (Krause 2007; Beck 2009). These facts imply other structured components of GMF in the halo of our galaxy. This effect to

HECR propagation in the Galaxy should be considered and it is a next target of our studies.

In a real situation, HECRs are deflected by not only GMF but also IGMF. However, our current understanding about IGMF is poor and IGMF modellings have large uncertainty. A numerical simulation on cosmological structure formation in local Universe showed a magnetic structure highly concentrated to dense region (Dolag et al. 2005). In this case, HEPs are almost not deflected except the directions of clusters of galaxies, since the cross-sectional area occupied by strong IGMF is small. A simple modelling of IGMF by Takami et al. (2006) also predicted relatively small deflection angles of HEPs and showed that HEP sources are unveiled by HEPs themselves within a few degree (Takami & Sato 2008a). These 2 IGMF models are based on a realistic matter structure of local Universe constructed by the IRAS catalog of galaxies. On the other hand, hydrodynamical simulations on cosmological structure formation predicted relatively strong IGMF in filamentary structures up to 10nG (Sigl et al. 2004; Das et al. 2008). A large cross-sectional area of filamentary structures with $\sim 10$ nG fields makes HEPs be deflected significantly and a large part of information on their sources is lost. Note that these IGMFs have uncertainty on observer's positions because their resultant matter distributions do not correspond to local Universe actually observed. However, an IGMF model of Das et al. (2008) does not lose the correlation between the arrival directions of HEPs and large-scale structure of nearby Universe (Ryu et al. 2009). Moreover, another modelling of IGMF pointed out the possibility of fake correlation, which means that HECRs are scattered at strongly magnetized region not including their sources (Kotera & Lemoine 2008). In this case, the correlation with large-scale structure may be also conserved. Thus, it is uncertain at present because of the uncertainty of IGMF itself whether IGMF disturbs possible correlation between the arrival directions of HEPs and the positions of their sources, though the correlation with the large-scale structure is expected by many works. One possibility to know IGMF structure is a project of Faraday rotation measurement by Square Kilometer Array [3]. The Faraday rotation on the whole sky will give us useful information on magnetic fields in our local Universe.

In this study, we discussed the effects of GMF in cosmic ray astronomy. As we briefly discussed in this section, the understanding of the heavy components in HECRs and IGMF will be a key to investigate the potential of cosmic ray astronomy.

H.T. thanks to Veniamin Berezinsky for useful comments at the early stage of this study and Peter Biermann for comments on GMF in the Galactic halo. This work is supported by World Premier International Research Center Initiative (WPI Initiative), the Ministry of Education, Culture, Sports, Science and Technology (MEXT) of Japan. This work is also supported by Grants-in-Aid for Scientific Research from the MEXT of Japan through No.21840019 (H.T.) and No.19104006 (K.S.).

REFERENCES

Abraham, J., et al. [The Pierre Auger Collaboration] 2007, Science, 318, 938
Abraham, J., et al. [The Pierre Auger Collaboration] 2008, Astropart. Phys., 29, 188
Allard, D., Parizot, E., Olinto, A.V., Khan, E., & Goriely, S., 2005, A&A, 443, L29
Alvarez-Muniz, J., Engel, R., Stanev, T. 2002, ApJ, 572, 185
Beck, R. 2009, Ap&SS, 320, 77
Bellido, J.A. et al. [The Pierre Auger Collaboration], Proc. 31th Int. Cosmic Ray Conf. (Lodz) #124
Belz, J., et al. [The HiRes Collaboration], Proc. 31th Int. Cosmic Ray Conf. (Lodz) #854
Bhattacharjee, P., & Sigl, G. 2000, Phys. Rep., 327, 109
Blake, C., Pope, A., Scott, D., & Mobasher, B. 2006, MNRAS, 368, 732
Blasi, P. & de Marco, D. 2004, Astropart. J., 20, 559
Cuoco, A., Hannestad, S., Haugbolle, T., Kachelriess, M., & Serpico, P. D. 2009, ApJ, 702, 825
Das, S., Kang, H., Ryu, D., & Cho, J. 2008, ApJ, 682, 29
Dolag, K., Grasso, D., Springel, V., & Tkachev, I. 2005, J. Cosmology Astropart. Phys., 01, 009
Everett J. E., Zweibel, W. G., Benjamin, R. A., McCammon, D., Rocks, L., & Gallagher III, J. S. 2008, ApJ, 674, 258
George, M. R., Fabian A. C., Baumgartner, W. H., Mushotzky, R. F., & Tueller, J. 2008, MNRAS, 388, L59
Ghisellini, G., Ghirlanda, G., Tavecchio, F., Fraternali, F., & Pareschi, G. 2008, MNRAS, 390, L88
Greisen, K. 1966, Phys. Rev. Lett., 16, 748
Hague, J. et al. [The Pierre Auger Collaboration] 2009, Proc. 31th Int. Cosmic Ray Conf. (Lodz) # 143
Han, J. L., & Qiao, G.J. 1994, A&A, 288, 759
Han, J.L. 2007, in IAU Symp. 242, Astrophysical Masers and Their Environments, ed. J.M.Chapman & W.A.Baan (Cambridge: Cambridge Univ. Press), 55
Harari, D., Mollerach, S., & Roulet, E. 1999, J. High Energy Phys., 08, 022
Kachelriess, M., & Semikoz, D. 2005, Astropart. Phys., 23, 486
Kachelriess, M., Serpico, P. D., Teshima, M. 2007, Astropart. Phys., 26, 378
Kalashev, O. E., Kuz'min, V. A., & Semikoz, D. V. 2001, Mod. Phys. Lett., 16, 2505
Kashti, T. & Waxman, E. 2008, J. Cosmology Astropart. Phys., 05, 009
Kotera, K. & Lemoine, M. 2008, Phys. Rev. D, 77, 123003
Krause, M. 2007, Mem. Soc. Astron. Ital., 78, 314
Medina-Tanco, G. A., de Gouveia dal Pino, E. M., & Horvath, J. E. 1998, ApJ, 492, 200
Moskalenko, I. V., Stawarz, L., Porter, T. A., & Cheung, C. C. 2009, ApJ, 693, 1261
Mucke, A., Engel, R., Rachen, J. P., Protheroe, R. J., & Stanev, T. 2000, Com. Phys. Comm., 124, 290
Nonaka, T. et al. [The Telescope Array Collaboration], Proc. 31th Int. Cosmic Ray Conf. (Lodz) #974
Prouza, M., Smida, R. 2003, A&A, 410, 1
Ryu, D., Kang, H., & Das, S., Proc. 31th Int. Cosmic Ray Conf. (Lodz) #839
Saunders, W. et al. 2000, MNRAS, 317, 55
Sigl, G., Miniati, F., & Ensslin, T.A. 2004, Phys. Rev. D, 70, 043007
Sommers, P. 2001, Astropart. Phys., 14, 271
Stanev, T. 1997, ApJ, 479, 290
Takami, H., Nishimichi, T., Yahata, K., & Sato, K. 2009, J. Cosmology Astropart. Phys., 06, 031
Takami, H. & Sato, K. 2008a, ApJ, 678, 606
Takami, H. & Sato, K. 2008b, ApJ, 681, 1279
Takami, H., & Sato, K. 2009, Astropart. Phys., 30, 306
Takami, H., Yoshiguchi, H., & Sato, K. 2006, J. Cosmology Astropart. Phys., 639, 803, [Erratum ibid. 653 (2006) 1584]
Takeda, M., et al. [The AGASA Collaboration] 1999, ApJ, 522, 225
Takeuchi, T. T., Yoshikawa, K. & Ishii, T. 2003, ApJ, 587, L89 (erratum ibid. 606 (2004) L171)
Tinyakov, P. G., Tkachev, I. I. 2002, Astropart. Phys., 18, 165
Tinyakov, P. G., & Tkachev, I.I. 2005, Astropart. Phys., 24, 32
Torres, D.& Anchordoqui, L. 2004, Rep. Prog. Phys. 67, 1663
Yoshiguchi, H., Nagataki, S., & Sato, K. 2003, ApJ, 596, 1044
Yoshiguchi, H., Nagataki, S., & Sato, K. 2004, ApJ, 607, 840
Zatsepin, G.T., & Kuz'min, V.A. 1966, JETP Lett., 4, 78

[3] http://www.skatelescope.org/